C.P. No. 553

C.P. No. 553

MINISTRY OF AVIATION

AERONAUTICAL RESEARCH COUNCIL

CURRENT PAPERS

Free-Flight Measurements of the Zero-Lift Drag and Base Pressure on a Wind Tunnel Interference Model (M = 0.8 - 1.5)

by

G. H. Greenwood

LONDON: HER MAJESTY'S STATIONERY OFFICE

1961

PRICE 3s. 6d. NET

C.P. No. 553

U.D.C. No. 533.6.071.4:533.69.048.2

November, 1960

FREE-FLIGHT MEASUREMENTS OF THE ZERO-LIFT DRAG AND BASE PRESSURE ON A WIND TUNNEL INTERFERENCE MODEL (M = 0.8-1.5)

by

G. H. Greenwood

SUMMARY

Five free-flight models were flown to measure the zero-lift drag and body base pressure on a standard wind tunnel interference model over a Mach number range of 0.84 to 1.48.

Roughness bands on the wings and body of the model are shown to produce a small but definite increase in the zero-lift drag at all Mach numbers.

The measured drag is in fair agreement with corresponding measurements made in various transonio tunnels with differences that could plausibly be explained as the effects of tunnel interference.

The effect of a simulated wind tunnel support sting is shown to increase the base pressure. The discrepancy between models with and without a sting is greatest at subsonic speeds and progressively decreases with increasing Mach number until at M = 1.4 the sting has no effect on base pressure.

The roughness bands consisted of carborundum grains in a matrix of aluminium paint rolled on to the surface. Although the nominal size of grain used was 0.003 inches measurements showed that the effective mean grain height was 0.0026 inches above the paint surface and 0.0029 inches above the unpainted surface.

Previously issued as R.A.E. Tech. Note No. Aero 2725 - A.R.C.22,711.

LIST OF CONTENTS

LIST OF ILLUSTRATIONS

LIST OF ILLUSTRATIONS (Contd.)

1 INTRODUCTION

The tests described in this note were made as part of a combined wind tunnel/free-flight model programme to investigate the nature and extent of wall interference effects in transonic tunnels[1]. In this programme the rôle of the free-flight models was to provide force and pressure measurements free from wall interference effects against which similar measurements, made in various transonic tunnels, could be compared.

The contribution of the free-flight models to the above programme was the measurement of zero-lift drag and body surface pressures and these measurements (obtained from model 2 of this note) have already been published in Ref.1*.

The purpose of this note is to describe the test methods used to obtain these results and to present some aspects of the results which are of interest but not necessarily relevant to the main programme of Ref.1.

Removed from the context of the comparisons of Ref.1, the pressure measurements on the body surface are of limited interest and are therefore not included in the present note although mention is made of the technique used to obtain them.

A standard model shape (with variations in scale) was used in all the tunnel and free-flight model tests but the addition of small fins to some of the free-flight models to provide directional stability was necessary.

An interesting aspect of the present tests is the well-defined sting interference effect on the body base pressure.

2 DESCRIPTION OF THE MODELS

2.1 Model configuration

The shape of the free-flight models was kept as close as possible to that of the configuration of Fig.1 and Table 1 which represents the standard shape tested in the transonic tunnels.

Five free-flight models were flown; four had a body diameter of 5 inches (Fig.2) and one had a body diameter of 1.75 inches and was mounted on a simulated tunnel support sting (Fig.3).

Certain deviations from the standard shape of Fig.1 were unavoidable on the 5-inch models in that fins were added to the body of each model to provide directional stability, and on two models a small pitot rake was added to the body in an attempt to clarify some anomalies in the base-pressure measurements (see section 4.3). The 1.75 inch sting-mounted model, however, was kept to the standard shape of Fig.1.

In order to avoid possible confusion resulting from boundary-layer transition movements the wind tunnel models had transition fixed at the wing leading edge and near the body nose. In order to try and achieve comparable boundary-layer flow conditions between the tunnel and free-flight models transition was fixed on the sting-mounted free-flight model and on two of the 5 inch models (2 and 4). This was achieved by applying roughness bands in the positions shown in Fig.2. Two 5 inch models (1 and 3) were flown without roughness bands as a comparison.

---

*Measurements of aerodynamic-centre position and lift-curve slope were also made by free-flight models for the programme of Ref.1 but are to be reported separately.

The free-flight models tested and their respective functions are summarised below; the 5 inch models will be referred to as the "separating" models and the 1.75 inch model as the "non-separating" model*.

(a) Separating models

Model 1. Smooth model; to measure zero-lift drag and body-surface and base pressures.

Model 2. Roughness bands on body and wings; to measure zero-lift drag and body-surface and base pressures.

Model 3. Smooth model; to measure boundary-layer profile, body base pressure and zero-lift drag.

Model 4. Roughness bands on body and wings; to measure boundary-layer profile, body base pressure and zero-lift drag.

(b) Non-separating model

Model 5. Roughness bands on body and wings; to measure body-surface and base pressures. Model had simulated tunnel support sting.

2.2 Model construction

(a) Separating models

Three major components were used in the construction of the separating models, a brass nose portion, a 5 inch diameter light-alloy cylindrical body and high density compressed wood wings.

The telemetry equipment was carried in the light-alloy body with aerials consisting of copper strips recessed into the wings.

(b) Non-separating model

This model was machined entirely from light alloy; the model body and sting were of solid section the body being slotted to take the wings which were cemented and pinned into position. Because of its smaller scale no equipment could be carried in the body of the model and so a separate housing for the telemetry equipment was provided on the nose of the boost motor (Fig.3). The pressure lines from the body surface and base were routed to the telemetry housing in recesses milled into the sting surface: these were finally filled and smoothed to the sting contour.

3 TEST TECHNIQUES

3.1 Boosting technique: Separating models

Each model was mounted in tandem on a 6.8 inch diameter fin stabilised rocket motor (Fig.7) which boosted it to the required test velocity. At all-burnt the model separated from the boost assembly and followed its own trajectory: during this period all the flight measurements were made.

3.2 Boosting technique: Non-separating model

In this design the model was rigidly attached to its rocket motor and no model-from-rocket separation occurred. The 5 inch diameter rocket motor was covered by a compressed paper tube which served as an attachment for the stabilising fins and also ensured a clean air flow over the configuration (Fig.6).

---

*See sections 3.1 and 3.2.

3.3 Flight measurements: Separating models

The instrumentation of the separating models to obtain the necessary force and pressure measurements was:

Models 1 and 2

12 pressure transducers for body-surface pressure measurements;
2 pressure transducers for body base-pressure measurements;
1 longitudinal accelerometer.

Models 3 and 4

6 pressure transducers for body base-pressure measurements;
5 pressure transducers for the boundary-layer pitot pressure survey;
1 pressure transducer for body-surface static pressure measurement in plane of pitot rake;
2 longitudinal accelerometers.

The pressure transducers were all of the bellows type. One side of the bellows of each transducer was connected by a copper tube to its appropriate measuring station and the other side of the bellows was connected to a common reference-pressure chamber which was sealed at the known atmospheric pressure immediately prior to launching. Pressure measurements were thus obtained as values referenced to the known pressure in the common chamber.

Trajectory and velocity were obtained from kinetheodolite observations and drag coefficients were obtained from the model-borne accelerometers using the methods of Refs.2 and 3.

3.4 Flight measurements: Non-separating model

Pressure measurements only were made on this model. The instrumentation used was as follows:-

8 pressure transducers for body-surface pressure measurements;
2 pressure transducers for body base-pressure measurements.

Pressure measurements were obtained using the same method as on the separating models, i.e. bellows-type transducers in conjunction with a sealed reference-pressure chamber.

Trajectory and velocity were obtained from radio Doppler and kinetheodolite observations.

4 DISCUSSION OF RESULTS

4.1 Zero-lift drag

The total zero-lift drag of all the separating models is shown in Fig.8.

Agreement between the two smooth models (1 and 3) and between the two roughened models (2 and 4) at supersonic speeds is as close as one can expect bearing in mind the generally accepted uncertainties in the technique ($\pm 5\%$ in C_{D_o}). The greater differences in drag coefficient at subsonic speeds are a reflection of the small decelerations appropriate to this region and with currently available accelerometers uncertainties of up to 10% may occur.

The longer flight path of models 3 and 4, however, has allowed a greater measure of resolution of the drag at subsonic speeds and more weight has been given to the subsonic drag levels obtained from these models than to those from models 1 and 2.

The curves of Fig.8 include the drag of the small pitot rake on models 3 and 4 but this is estimated to be within the normally expected limits of uncertainty associated with free-flight drag measurements.

From the curves of Fig.8 mean drag curves relevant to the smooth and roughened models have been derived, using the drag obtained from models 3 and 4 to define the subsonic levels. These mean curves are compared in Fig.9 and the drag difference ΔC_{D_o} (representing the drag due to the presence of the roughness bands) is shown in Fig.10.

A comparison is made in Fig.11 between the zero-lift drag obtained from models 2 and 4 (roughness applied) and some of the tunnel results. All these results have been corrected to conditions representing free-stream static pressure on the body base. Fair agreement exists between the tunnel and free-flight models with differences that can plausibly be attributed to tunnel interference effects.

4.2 Effect of roughness bands on zero-lift drag

Comparison of the mean drag curves for the smooth and roughened models (Fig.9) suggests that the effect of roughness bands has been to increase the drag at all Mach numbers.

This drag increase, being derived from the results of four model flights, is adequately confirmed but the existence of some uncertainty particularly at subsonic speeds cannot be entirely discounted.

The possible inclusion of uncertainties in the curves of Fig.9 prohibits any attempt at a detailed analysis of roughness effects in terms of wing and body transition point movement; nevertheless, the existence of a drag increase of the magnitude shown in Fig.9 indicates the advisability of including roughness bands on free-flight drag models in order to reduce ambiguities where estimated skin-friction drag values are used to derive non-viscous drag components.

4.3 Body base-pressure and boundary-layer measurements (separating models)

The necessity to correct the total zero-lift drag curves to a form permitting direct comparison with the tunnel measurements, i.e. to conditions representing free-stream static pressure on the body base, entailed the measurement of base pressures on all the free-flight models.

It should be noted that the base of each separating model had a deep cavity concentric with the model axis into which the launching spigot was located when the model was on its boost motor. The base pressures were measured on the annulus surrounding this cavity and in the centre of the cavity itself (Fig.2).

On the first two models tested (1 and 2), body base pressures were measured at the two positions shown in Fig.2 and the results suggest that there is a significant difference in the derived base drag between the two models (Fig.12). This measured difference in drag can only be accepted as real by the assumption of substantial differences in the condition of the

body boundary layer between models 1 and 2*. The presence of the size of roughness grain (0.003 inches) on the body of model 2 seemed unlikely to induce a boundary-layer flow at the rear of the body significantly different from that on the smooth model at the Reynolds numbers of the tests (R_E = 26 to 41 millions based on body length) but in order to check this point and the general validity of the base-pressure measurements, two more models, 3 and 4, were flown.

Models 3 and 4 each had a pitot rake consisting of five pitot tubes mounted on the body surface as near to the base as possible (Figs.2 and 5) in order to survey the boundary layer. The results from these pitot surveys are plotted in Fig.15 and they confirm that the roughness strip has had no appreciable effect on the character of the boundary layer near the body base. This in turn suggests that the apparent difference in base drags measured on models 1 and 2 must arise from some peculiarity in the measurement or from a difference in the local flow conditions at the pressure measuring points. Some clue to these discrepancies is given by the more extensive base-pressure measurements of models 3 and 4 which show a scatter between individual measuring points of the same magnitude as the difference noted between models 1 and 2 (Fig.12). There is apparently no correlation between these variations and hole position, but one possible source of scatter is the occurrence of large and rapid fluctuations in the output of certain pressure transducers (Fig.14). These are obviously associated with corresponding pulsations in base flow but it is doubtful whether the bellows-type transducers used in this investigation have sufficiently high natural frequencies to reproduce such rapidly-fluctuating base pressures faithfully.

There was nothing in the results to suggest that the base pressure on the smooth models should be different from that on the roughened models and a mean value of base drag was therefore derived for each model (Fig.13a). From these mean values an overall mean base drag curve was drawn (Fig.13b) and used to convert the zero-lift drag results to conditions of zero base drag, thus enabling the drag comparison of Fig.11 to be made.

4.4 Effect of the simulated tunnel sting on base-pressure

The effect of the presence of the simulated tunnel support sting on the measured base pressure is shown in Fig.16 where the mean base pressure from all the separating models is compared with that obtained from the non-separating model.

The comparison is on the basis of measured C_P variation with Mach number and shows that at speeds below approximately M = 1.4 the base pressure has been increased by the presence of the sting; the greatest increase being at subsonic speeds where the increase has reduced the base drag by about 60% and the overall drag of the model by about 20%.

At approximately M = 1.4 the presence of the sting has no measurable effect on the base pressure.

---

*The possibility of small leakages between the model interior and base region cannot wholly be discounted as a source of body base-pressure differences between the models. Care was taken to ensure that such leakages should not occur, nevertheless, the high boosting accelerations may well have induced some distortion and hence leakage. The similarity in construction of the separating models would suggest that leakages of significantly different rates between the models would be unlikely; in the subsequent sections the effect of possible base leakages has therefore been considered negligible.

It should be noted that the separating models (i.e. without sting) all had stabilising fins on the body and the curves of Fig.16 include the possible influence of these fins on the base-pressure measurements; also the difference in size between the separating and non-separating models may have introduced a Reynolds number effect, but this is thought to be small.

5 CONCLUSIONS

(i) The values of zero-lift drag measured in these free-flight tests are in fair general agreement with corresponding transonic-tunnel measurements. Such differences as exist could plausibly be attributed to tunnel interference effects but no attempt has been made to analyse these effects in detail.

(ii) The existence of a well-defined increase in drag owing to the presence of roughness strips has been confirmed. This suggests that roughness bands should be incorporated on free-flight drag models when it is important to avoid uncertainties as to the state of the boundary layer.

(iii) The presence of the roughness bands appears to have little effect on the body boundary-layer profile and hence on the body base drag.

(iv) The effect of the presence of a simulated tunnel support sting was to increase the body base pressure at all Mach numbers but particularly at subsonic speeds where the increased base pressure resulted in a 60% reduction in base drag (equivalent to about 20% reduction in overall drag) compared with the no-sting case. A small extrapolation of the results indicates that at approximately M = 1.4 the base pressures with and without sting are equal.

LIST OF REFERENCES

No.	Author(s)	Title, etc.
1	O'Hara, F. Squire, L.C. Haines, A.B.	An investigation of interference effects on similar models of different size in various transonic tunnels in the U.K. A.R.C. 21,094. February, 1959.
2	Hamilton, J.A. Hufton, P.A.	Free flight techniques for high speed aerodynamic research. Journal of the Royal Aeronautical Society. March 1956.
3	Lawrence, T.F.C. Swan, J. Warren, C.H.E.	Development of a transonic research technique using ground-launched rocket-boosted models. Part II - Drag measurements. A.R.C. 14,167. March 1951.

TABLE 1

Particulars of standard model

Wing:

Gross aspect ratio	=	2.83
Gross taper ratio	=	0.333
Sweepback of mid-chord line	=	45°
Sweepback of leading edge	=	53.5°
Wing section	=	R.A.E. 102
Thickness/chord ratio	=	0.06

Body:

Overall fineness ratio	=	10.0

Nose is tangent circular arc ogive, with a tip radius of 0.025D, with fineness ratio of 3.6.

Afterbody is cylindrical.

All cross sections are circular.

Support sting:

Sting has constant taper, doubling its diameter in one model length from the base.

Ratio of sting diameter to model base diameter in plane of model base	=	0.8

WT.2078.C.P.553.63 - Printed in England

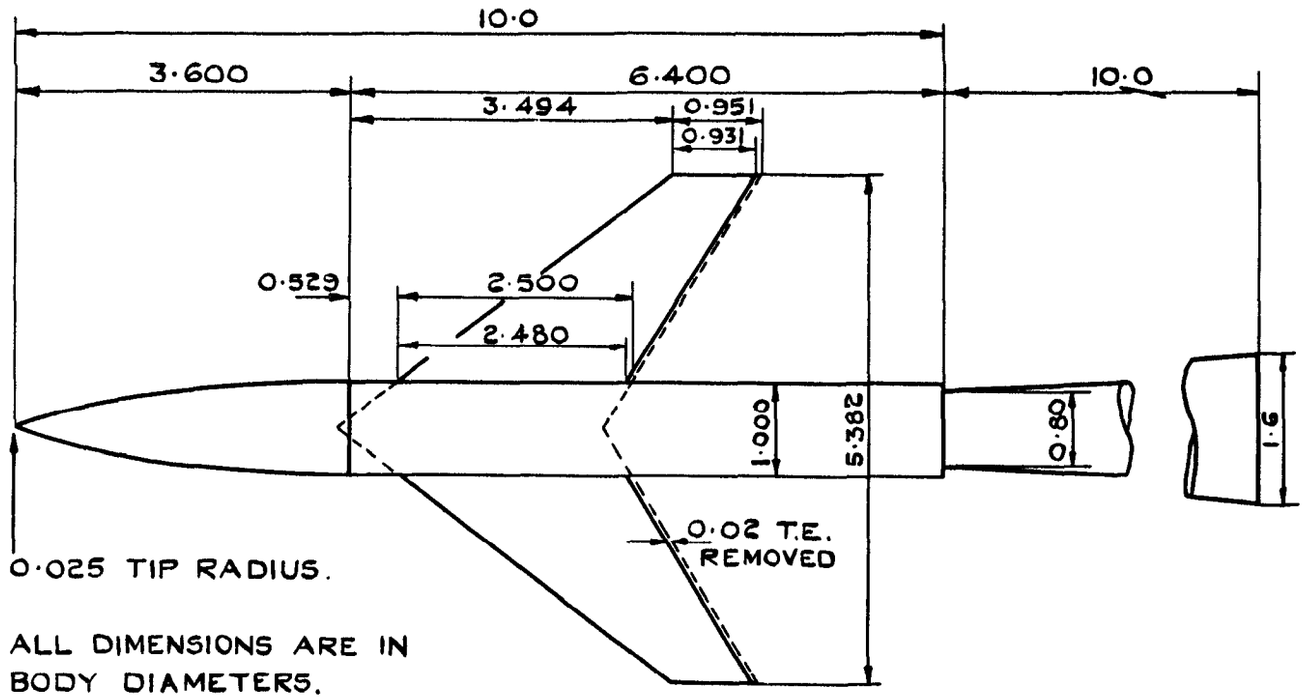

FIG. 1. DETAILS OF STANDARD MODEL & STING.

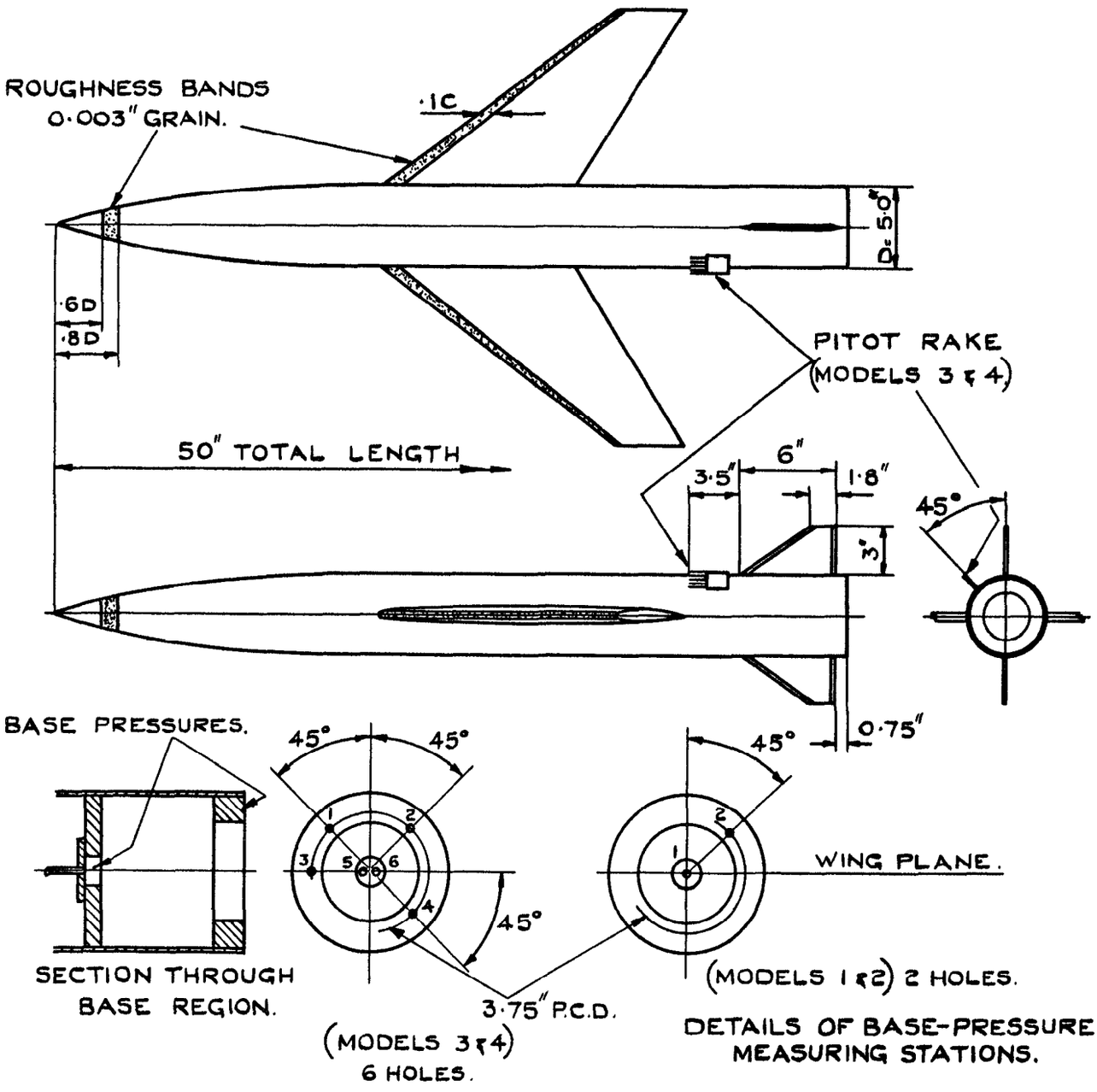

FIG. 2. DETAILS OF SEPARATING MODELS (1,2,3,4)

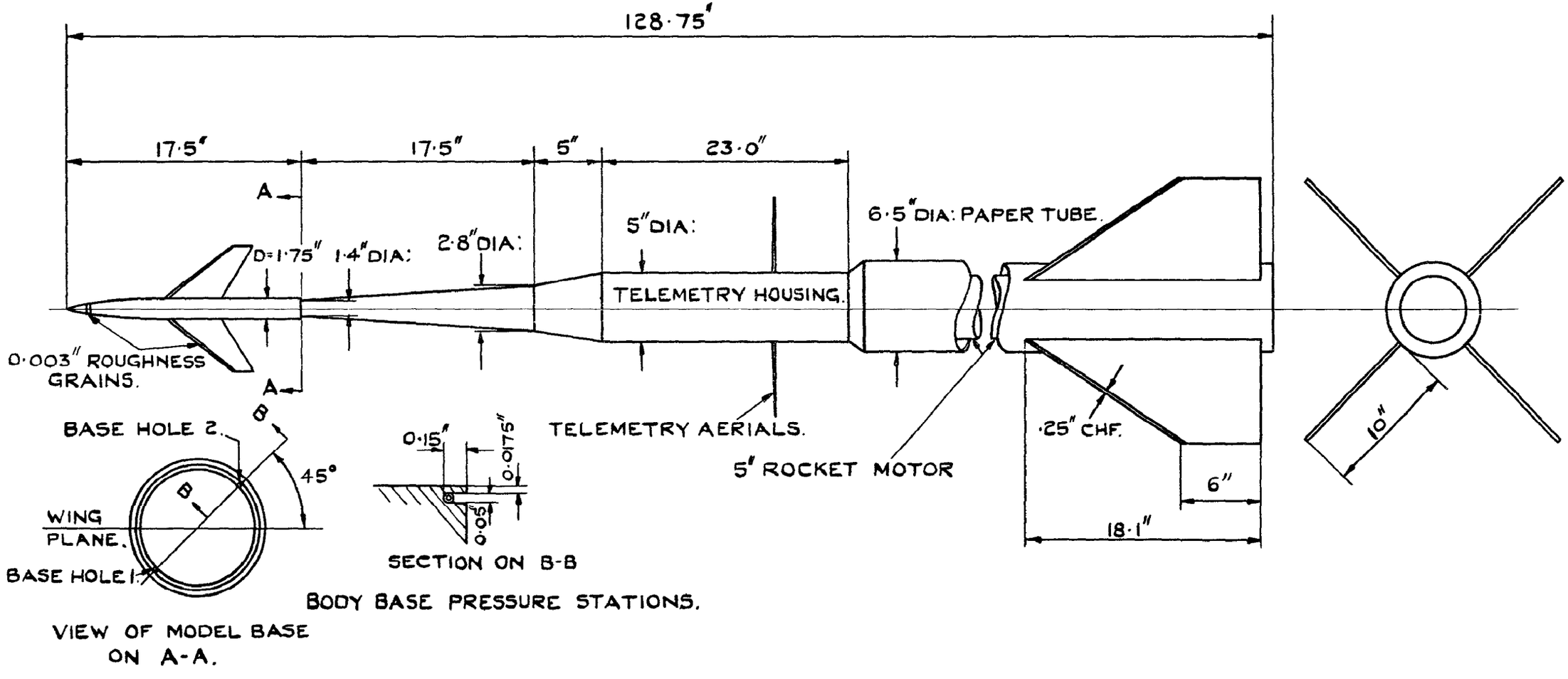

FIG. 3. DETAILS OF NON-SEPARATING MODEL (5.)

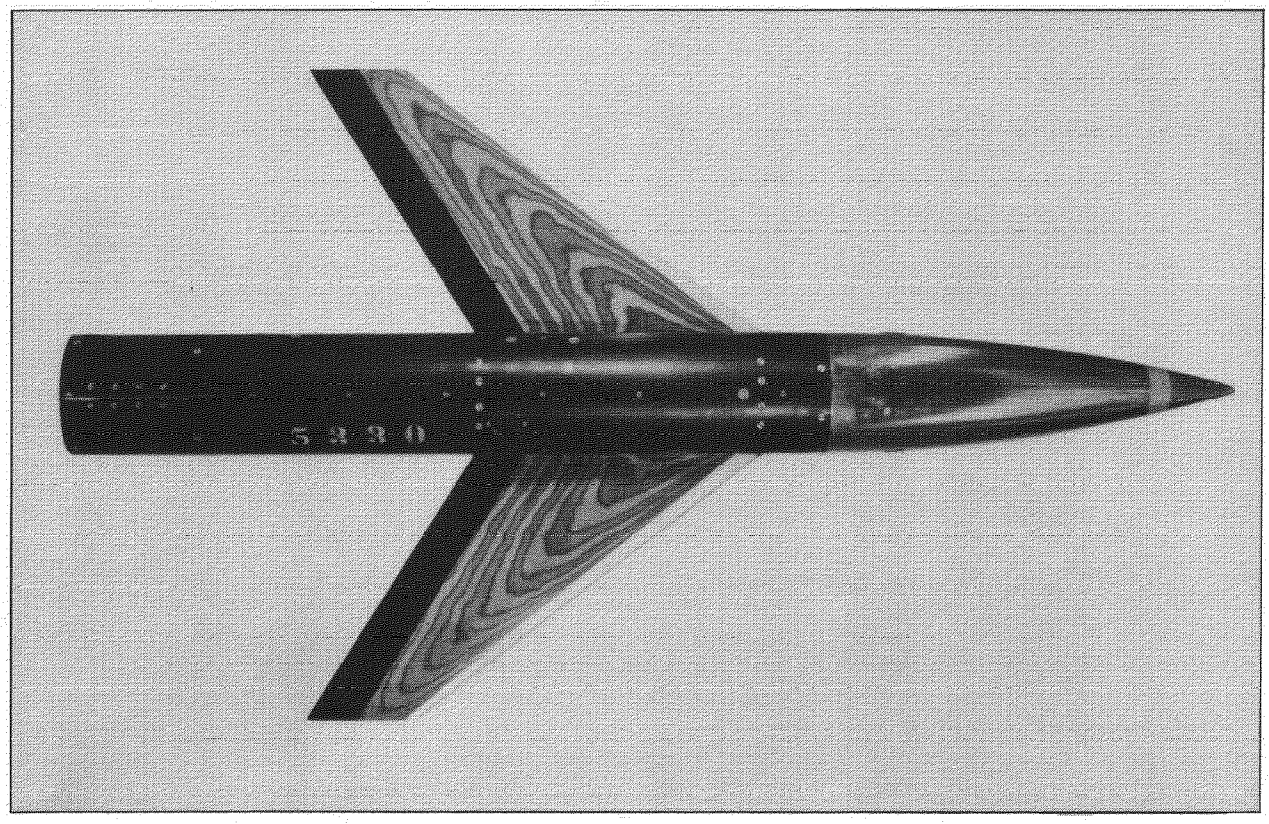

FIG. 4. SEPARATING MODEL

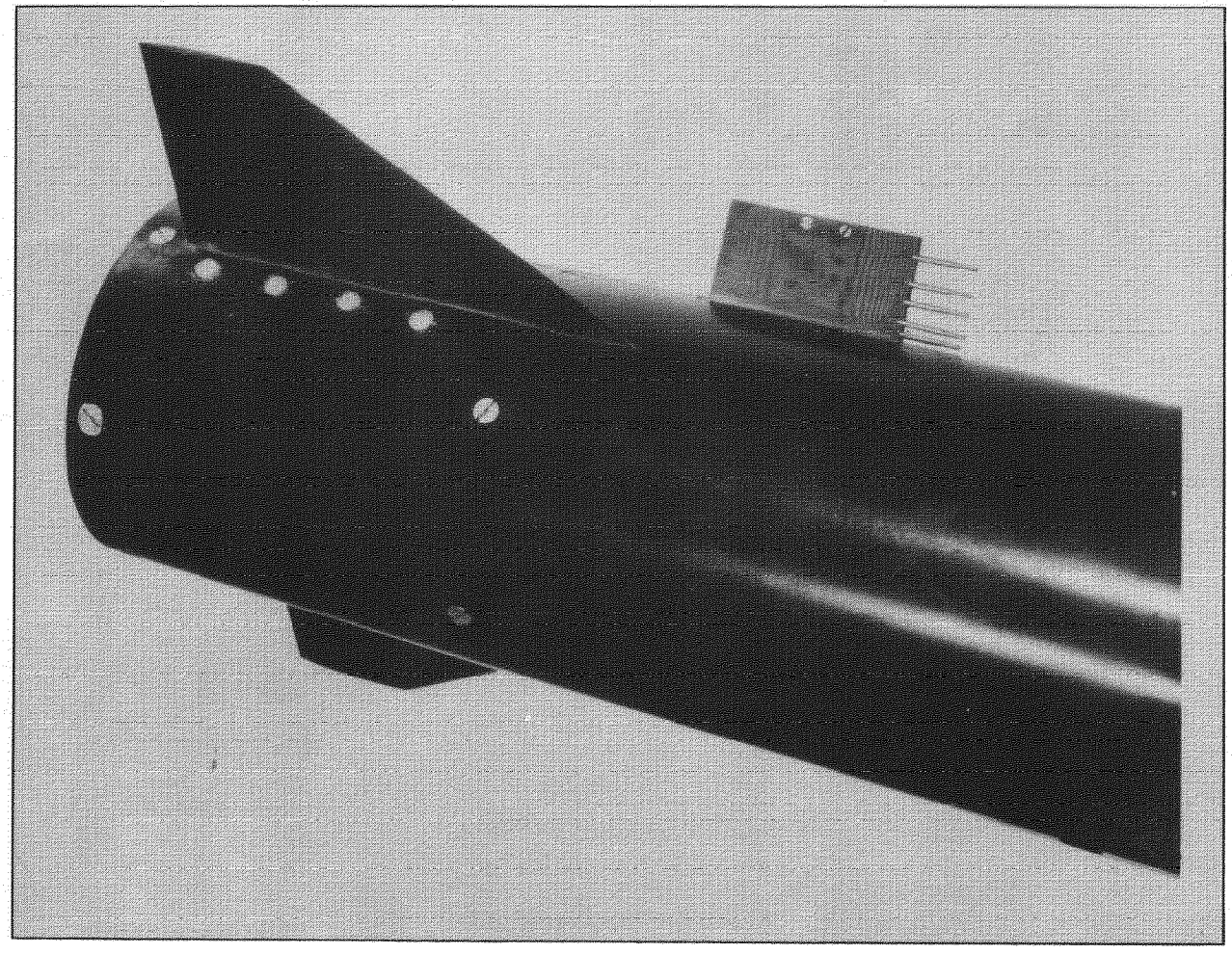

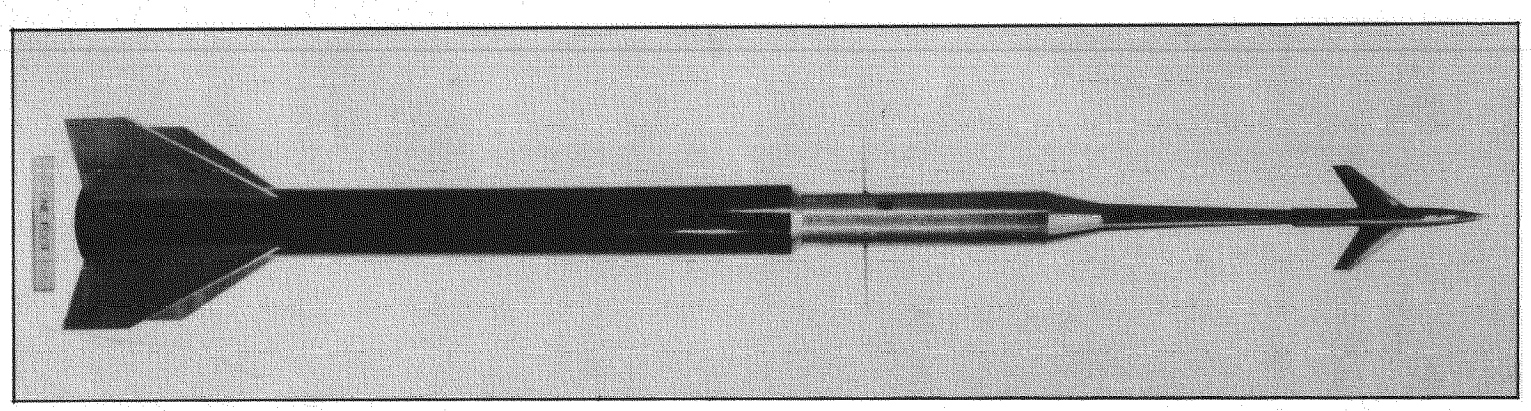

FIG. 6. NON-SEPARATING MODEL

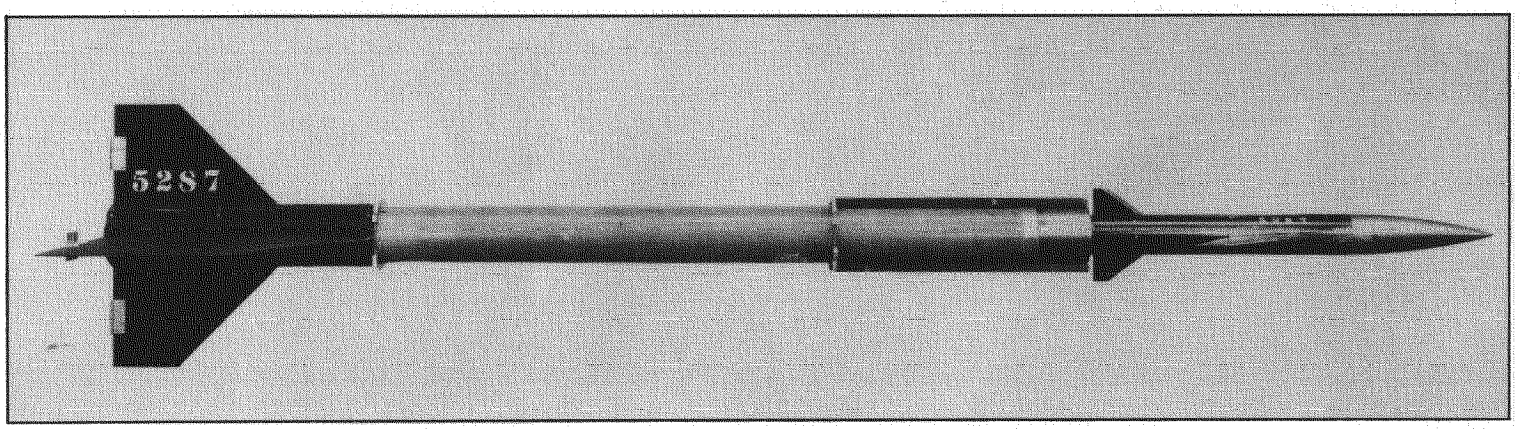

FIG. 7. BOOSTING ARRANGEMENT, SEPARATING MODELS

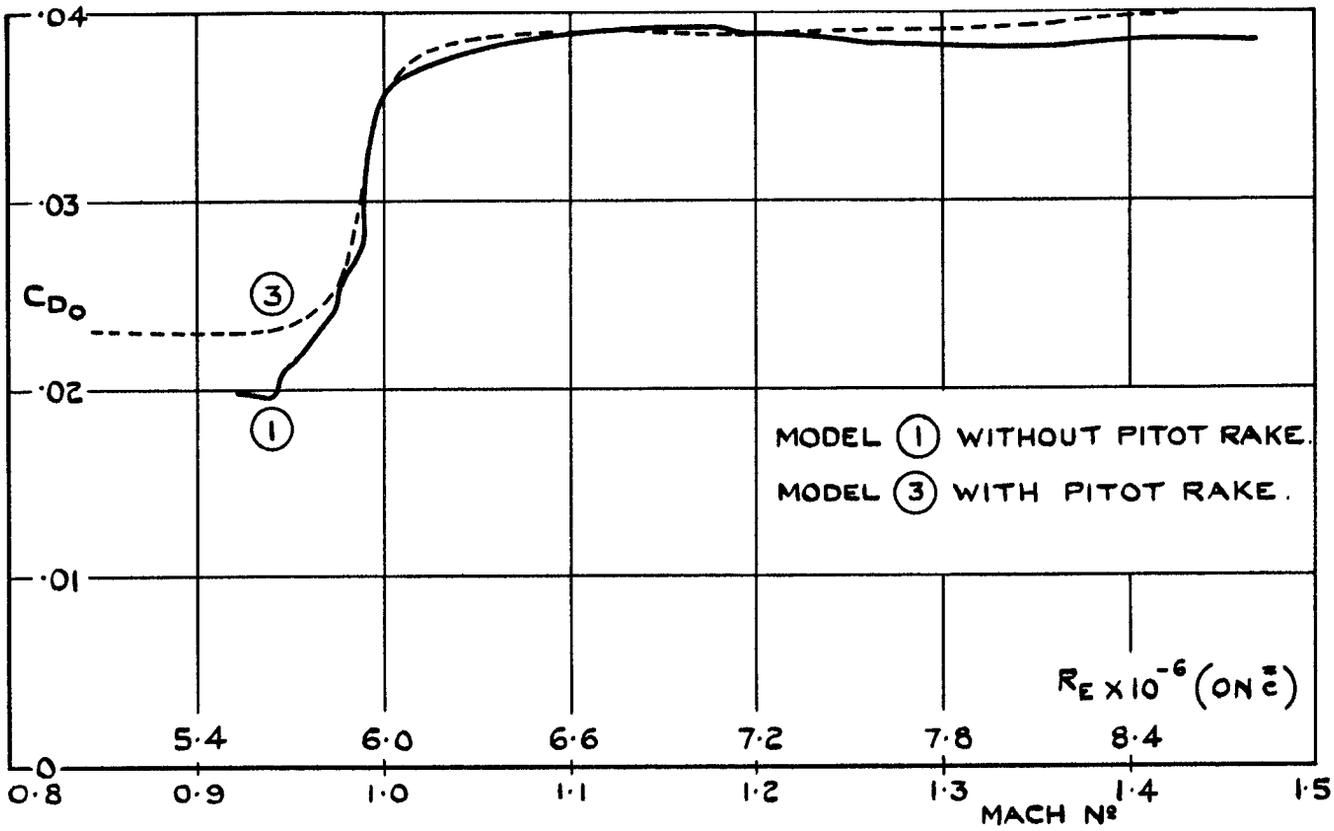

(a) ZERO-LIFT DRAG OF SMOOTH MODELS-1 & 3.

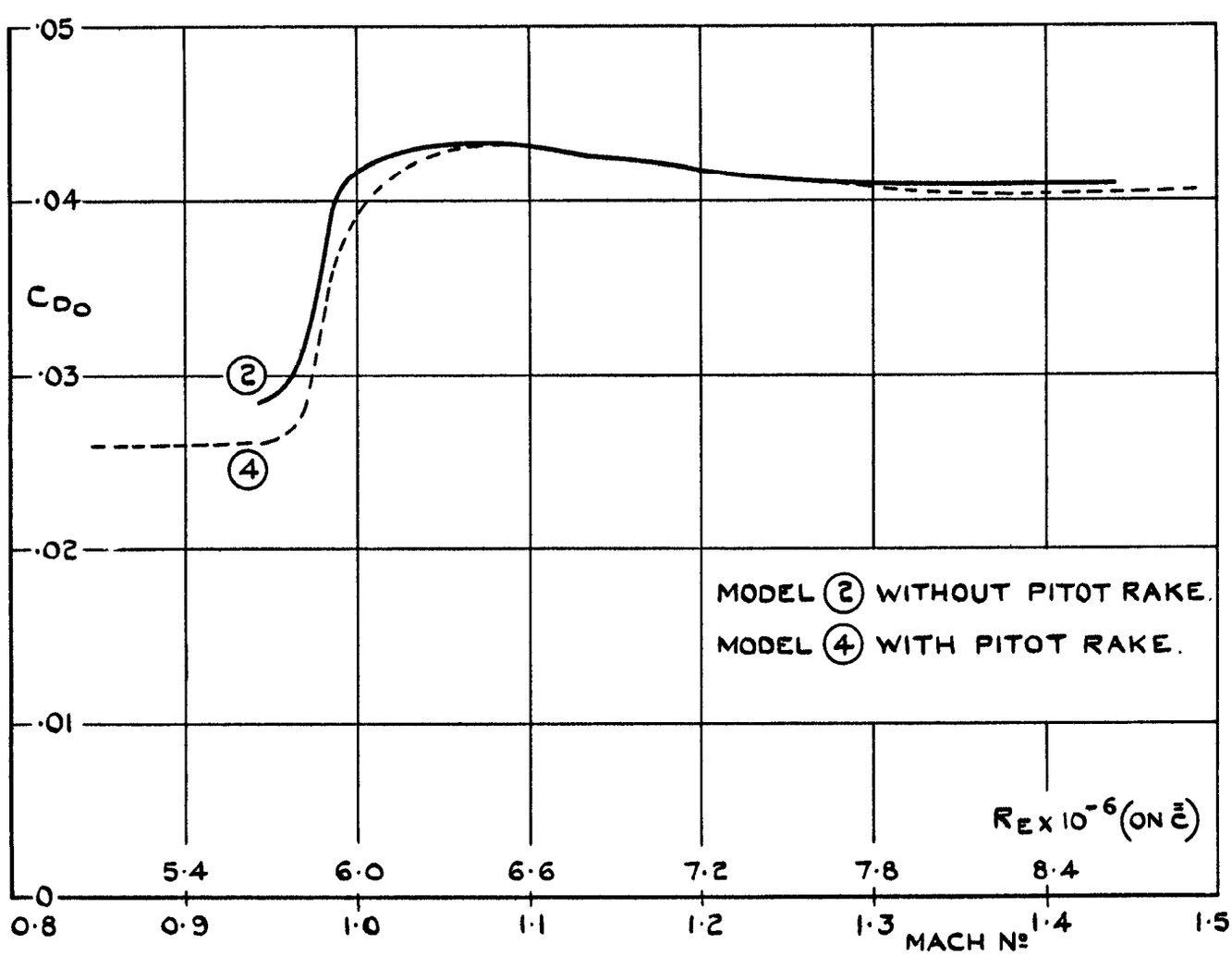

(b) ZERO-LIFT DRAG OF ROUGHENED MODELS-2 & 4.

FIG. 8. ZERO-LIFT DRAG - SEPARATING MODELS.

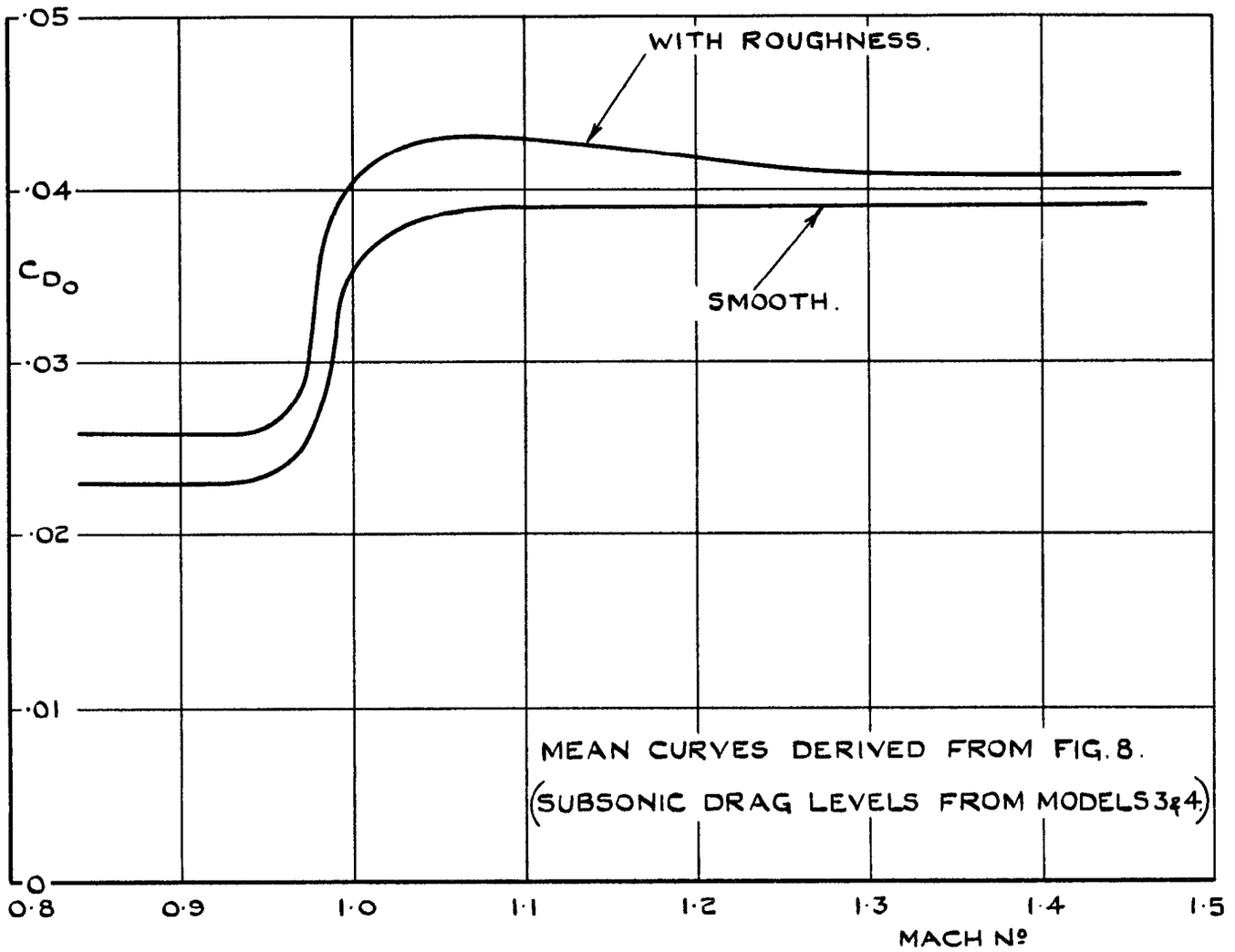

FIG. 9. COMPARISON OF ZERO-LIFT DRAG - SMOOTH AND ROUGHENED MODELS.

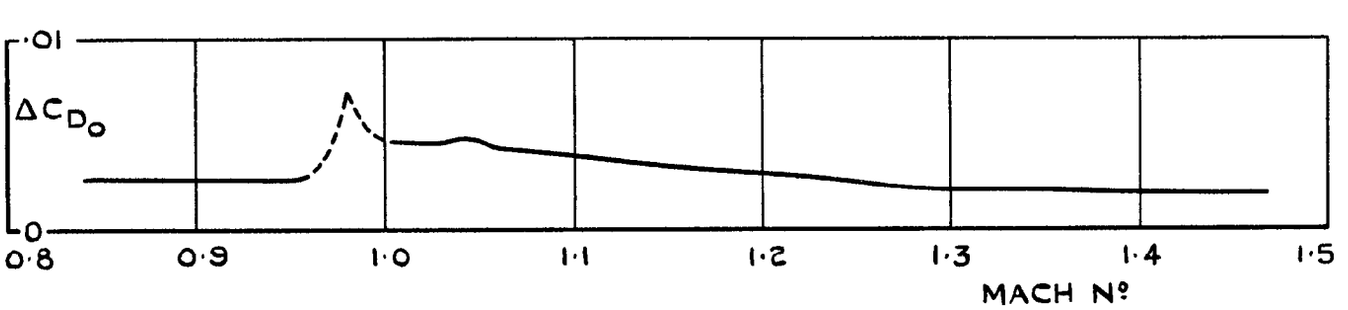

FIG. 10. DRAG INCREMENT DUE TO ROUGHNESS.

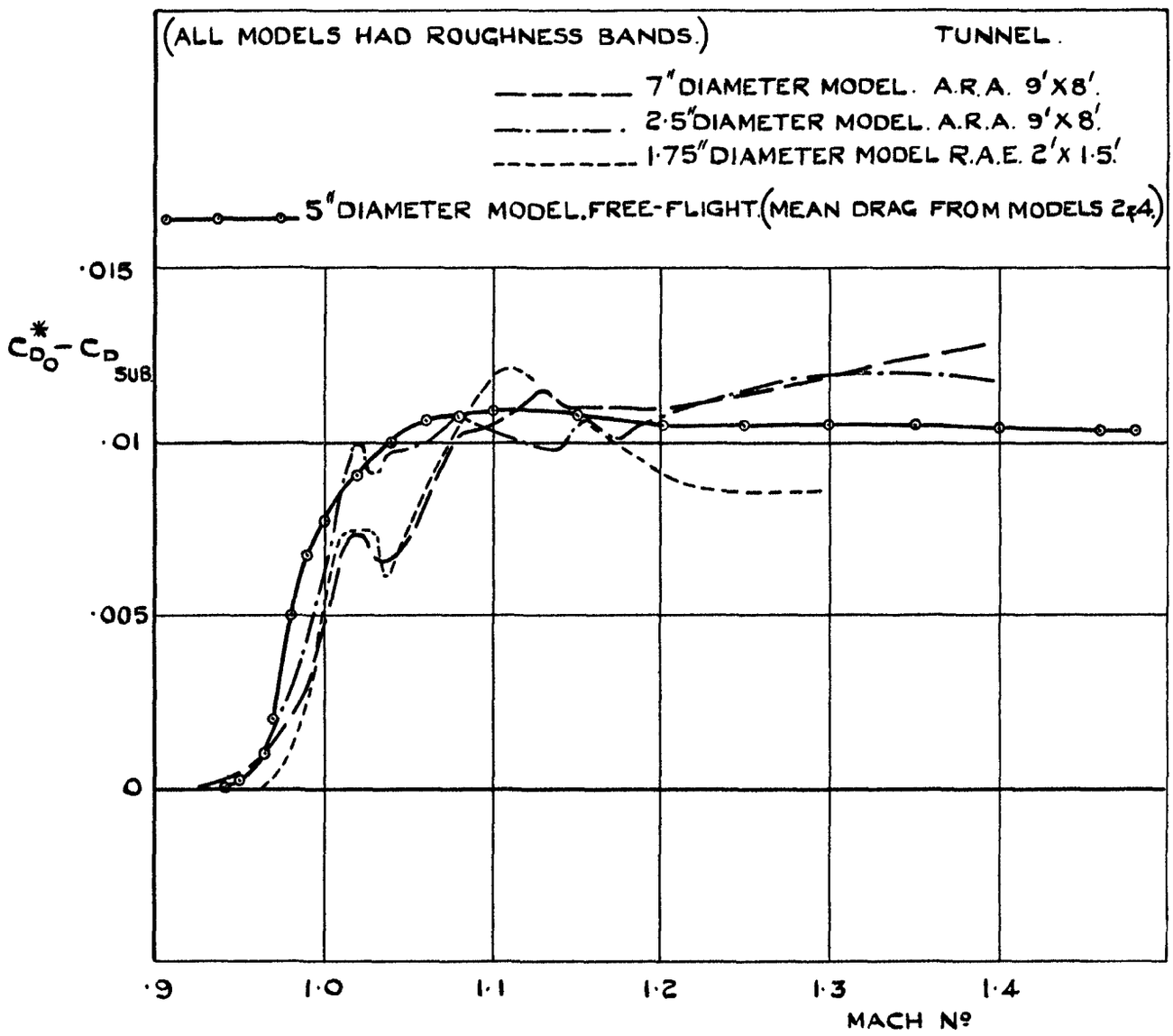

FIG. 11. COMPARISON OF TUNNEL & FREE-FLIGHT MEASUREMENTS OF ZERO-LIFT DRAG.

($C_{D_o}^*$ IS C_{D_o} FOR ZERO BASE DRAG.)

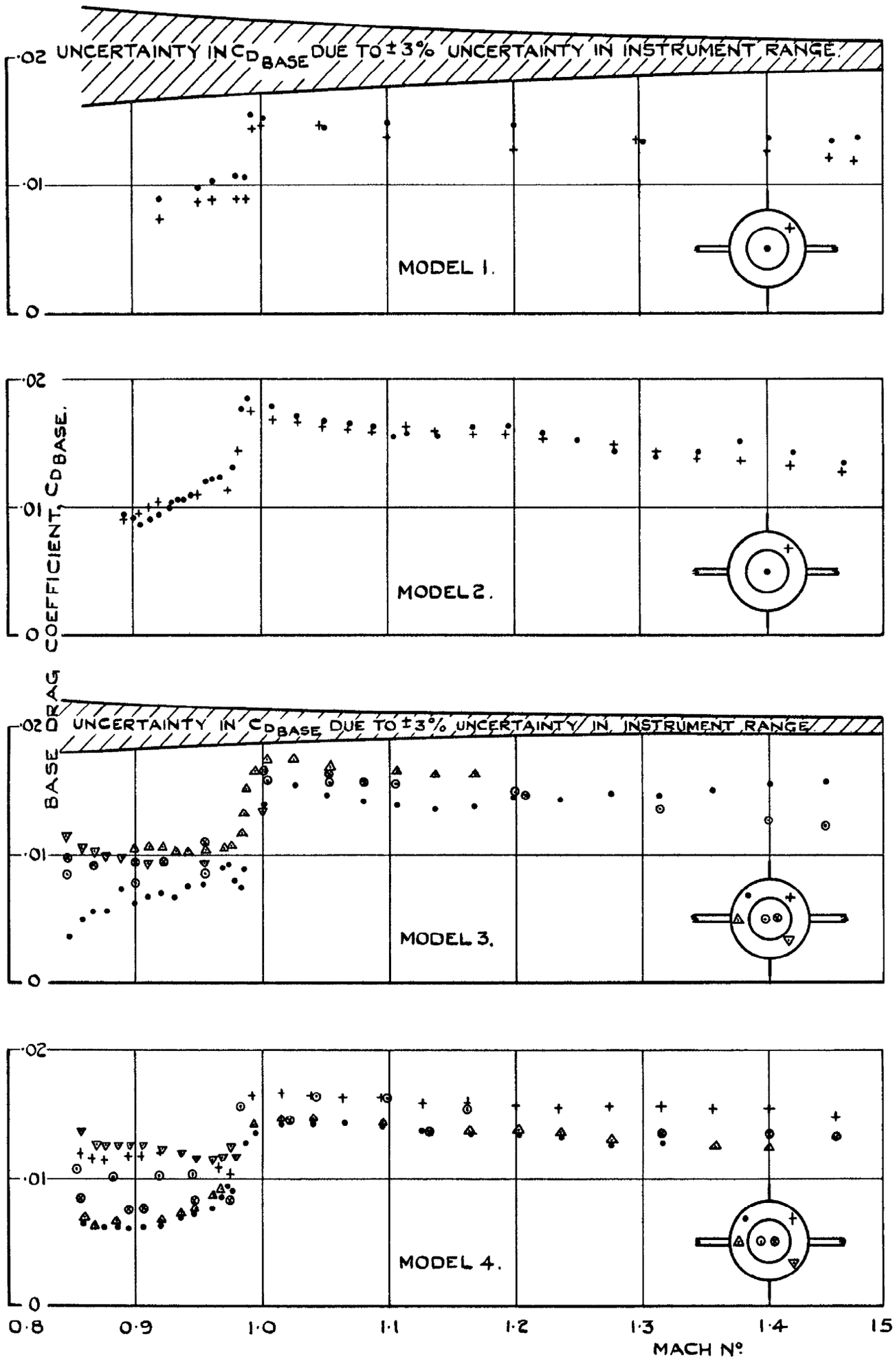

FIG.12. MEASURED BASE DRAG-SEPARATING MODELS.

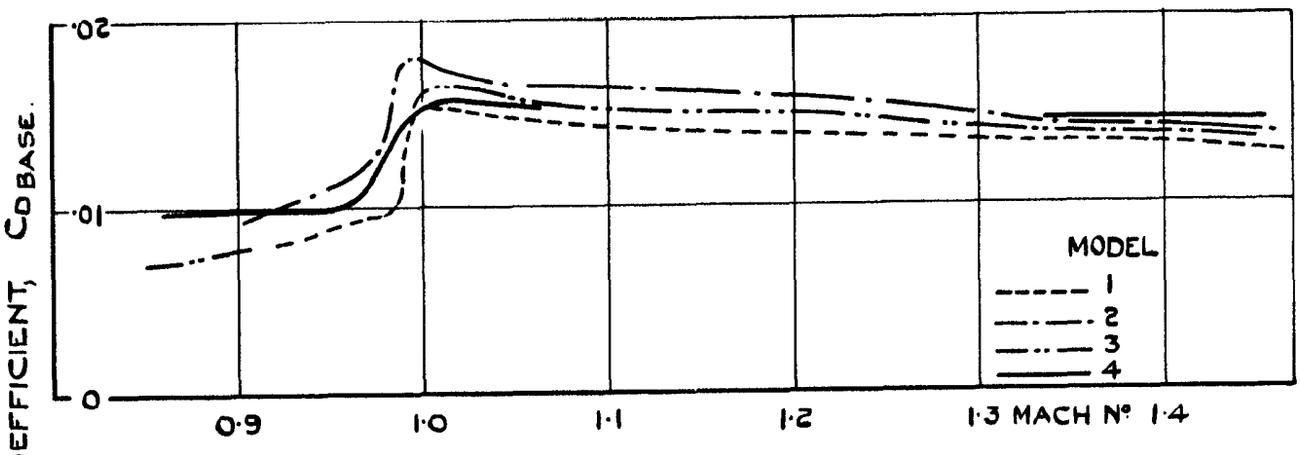

(a) COMPARISON OF MEAN BASE-DRAG COEFFICIENTS.

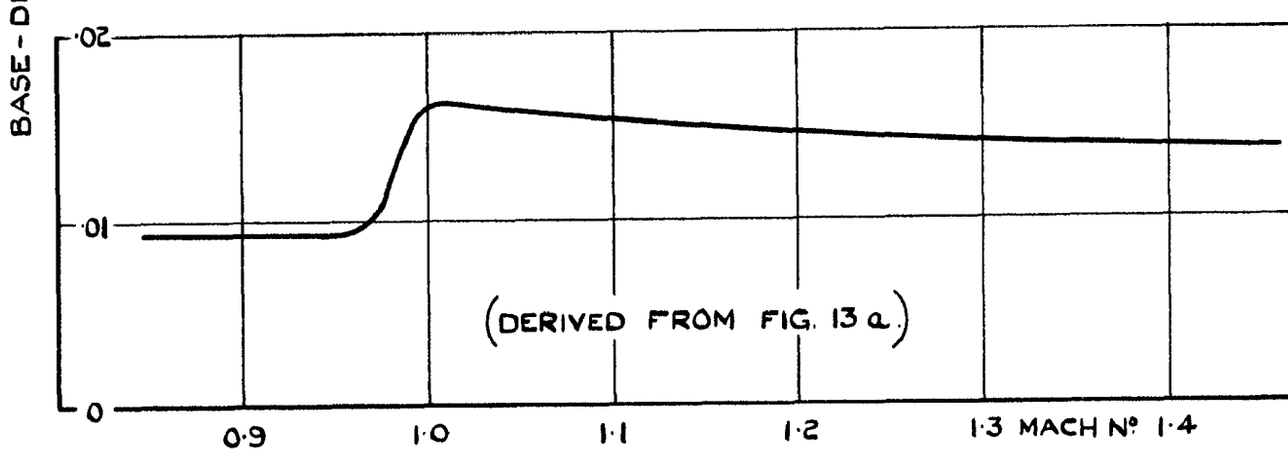

(b) DERIVED COMMON BASE-DRAG COEFFICIENTS.

FIG. 13. MEAN BASE DRAG-SEPARATING MODELS.

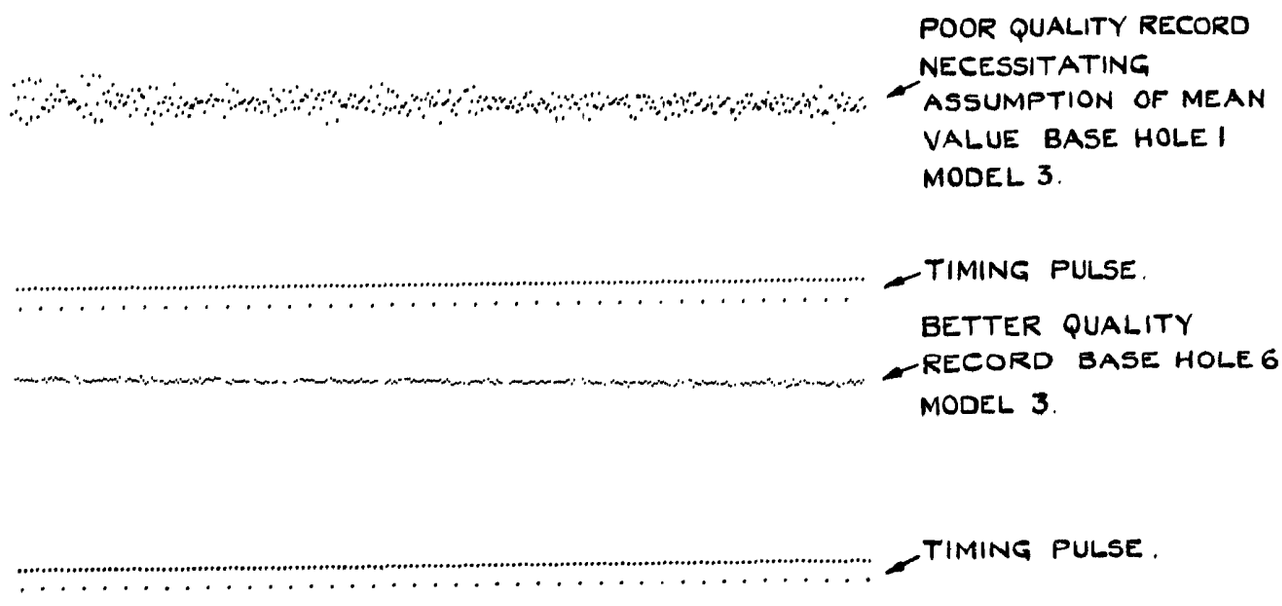

FIG. 14. TYPICAL BASE-PRESSURE TELEMETRY RECORD.

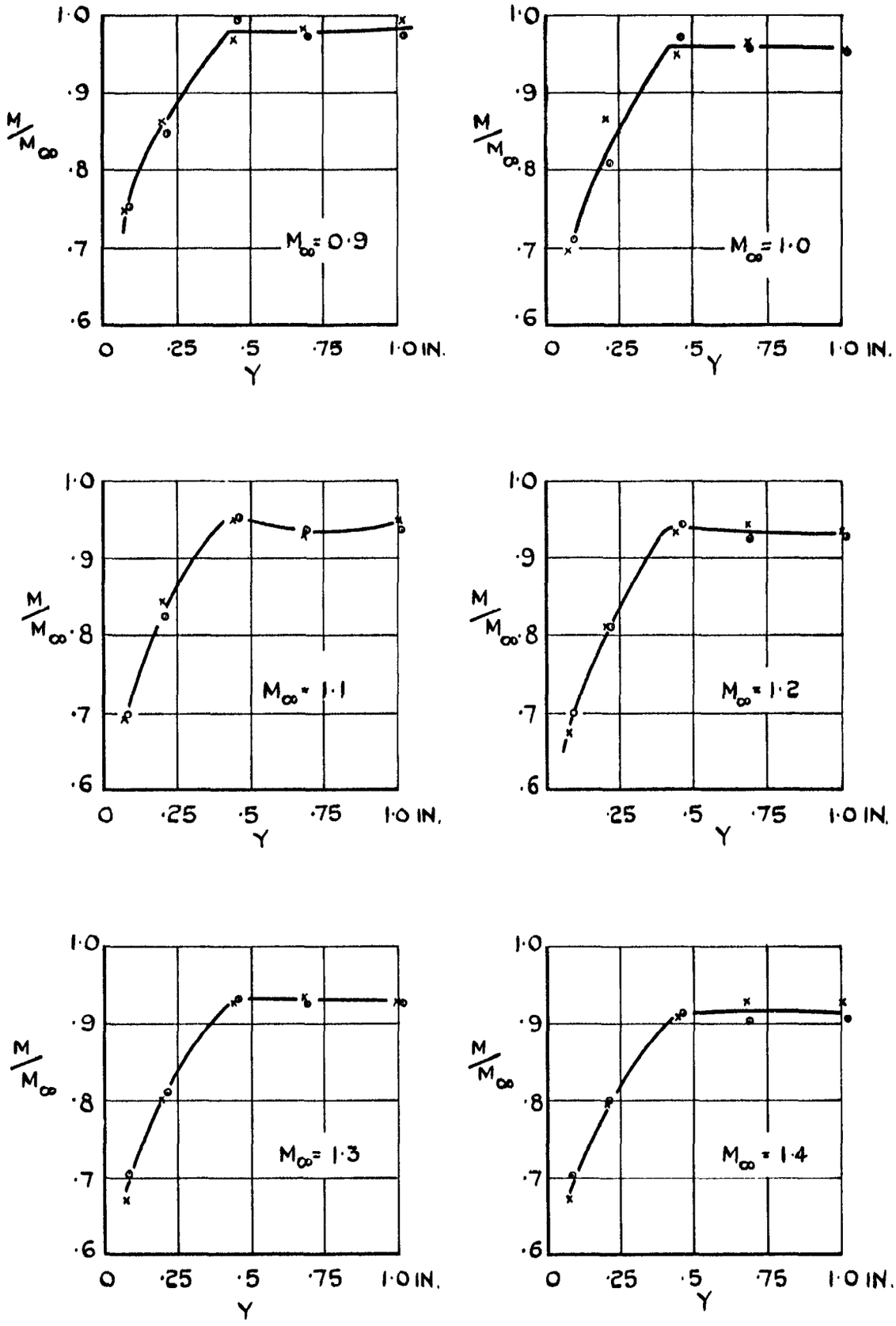

X = SMOOTH MODEL
⊙ = ROUGHENED MODEL.
M = MACH Nº IN THE BOUNDARY LAYER.
M_∞ = FREE-STREAM MACH Nº
Y = PERPENDICULAR DISTANCE FROM MODEL SURFACE (INCHES.)

FIG.15. BOUNDARY-LAYER PROFILES - MODELS 3 & 4.

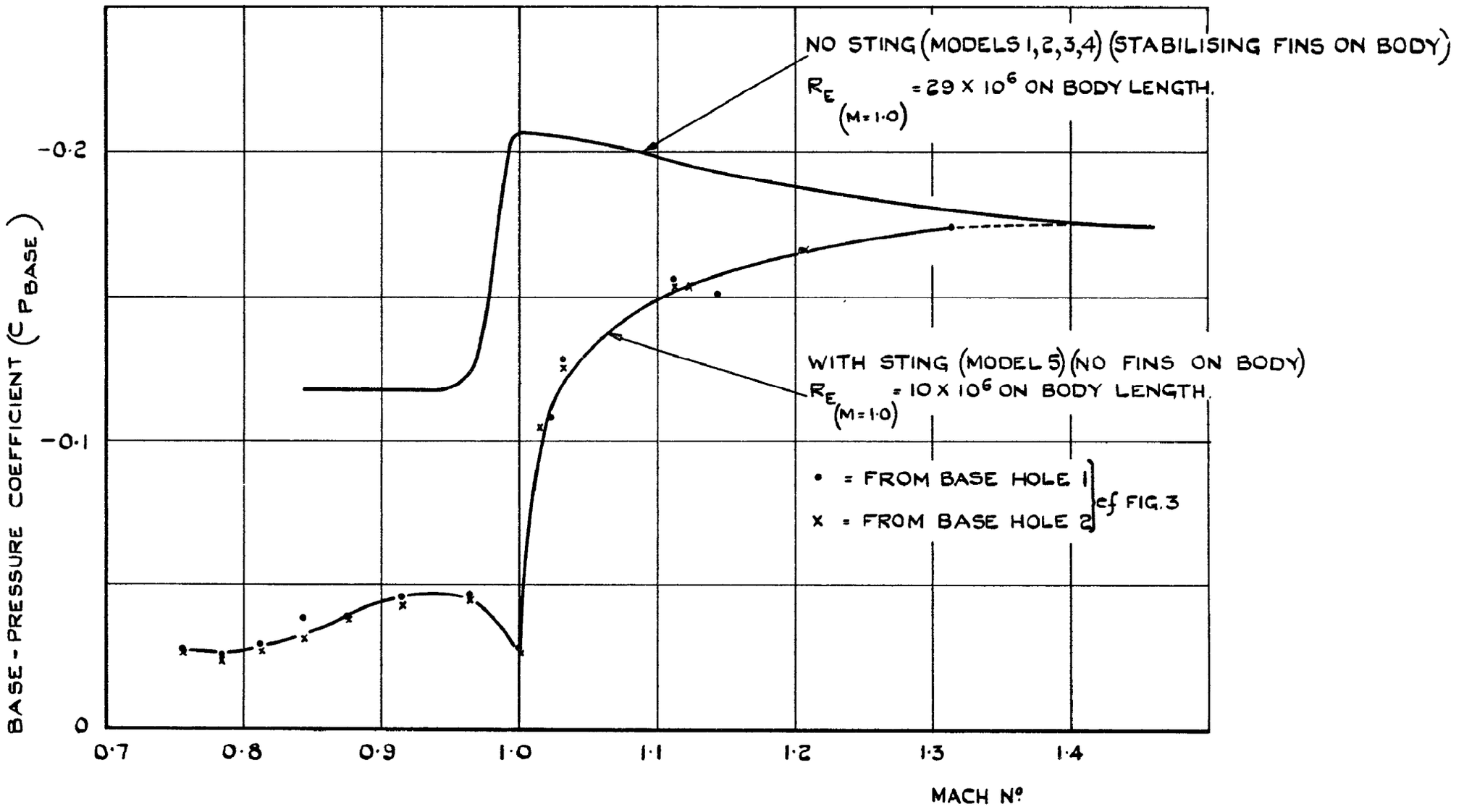
NO STING (MODELS 1,2,3,4) (STABILISING FINS ON BODY)
R_E (M=1·0) = 29 × 10⁶ ON BODY LENGTH.
WITH STING (MODEL 5) (NO FINS ON BODY)
R_E (M=1·0) = 10 × 10⁶ ON BODY LENGTH.
• = FROM BASE HOLE 1
x = FROM BASE HOLE 2
cf FIG. 3
BASE - PRESSURE COEFFICIENT ($C_{P_{BASE}}$)
−0·2
−0·1
0
0·7
0·8
0·9
1·0
1·1
1·2
1·3
1·4
MACH Nº

A.R.C. C.P. No.553

533.6.071.4:
533.69.048.2

FREE-FLIGHT MEASUREMENTS OF THE ZERO-LIFT DRAG AND BASE PRESSURE ON A WIND TUNNEL INTERFERENCE MODEL (M = 0.8-1.5).
Greenwood, G.H. Nov. 1960.

Five free-flight models were flown to measure the zero-lift drag and body base pressure on a standard wind tunnel interference model over a Mach number range of 0.84 to 1.48.

Roughness bands on the wings and body of the model are shown to produce a small but definite increase in the zero-lift drag at all Mach numbers.

(Over)

A.R.C. C.P. No.553

533.6.071.4:
533.69.048.2

FREE-FLIGHT MEASUREMENTS OF THE ZERO-LIFT DRAG AND BASE PRESSURE ON A WIND TUNNEL INTERFERENCE MODEL (M = 0.8-1.5).
Greenwood, G.H. Nov. 1960.

Five free-flight models were flown to measure the zero-lift drag and body base pressure on a standard wind tunnel interference model over a Mach number range of 0.84 to 1.48.

Roughness bands on the wings and body of the model are shown to produce a small but definite increase in the zero-lift drag at all Mach numbers.

(Over)

A.R.C. C.P. No.553

533.6.071.4:
533.69.048.2

FREE-FLIGHT MEASUREMENTS OF THE ZERO-LIFT DRAG AND BASE PRESSURE ON A WIND TUNNEL INTERFERENCE MODEL (M = 0.8-1.5).
Greenwood, G.H. Nov. 1960.

Five free-flight models were flown to measure the zero-lift drag and body base pressure on a standard wind tunnel interference model over a Mach number range of 0.84 to 1.48.

Roughness bands on the wings and body of the model are shown to produce a small but definite increase in the zero-lift drag at all Mach numbers.

(Over)

A.R.C. C.P. No.553

533.6.071.4:
533.69.048.2

FREE-FLIGHT MEASUREMENTS OF THE ZERO-LIFT DRAG AND BASE PRESSURE ON A WIND TUNNEL INTERFERENCE MODEL (M = 0.8-1.5).
Greenwood, G.H. Nov. 1960.

Five free-flight models were flown to measure the zero-lift drag and body base pressure on a standard wind tunnel interference model over a Mach number range of 0.84 to 1.48.

Roughness bands on the wings and body of the model are shown to produce a small but definite increase in the zero-lift drag at all Mach numbers.

(Over)

The measured drag is in fair agreement with corresponding measurements made in various transonic tunnels with differences that could plausibly be explained as the effects of tunnel interference.

The effect of a simulated wind tunnel support sting is shown to increase the base pressure. The discrepancy between models with and without a sting is greatest at subsonic speeds and progressively decreases with increasing Mach number until at M = 1.4 the sting has no effect on base pressure.

The measured drag is in fair agreement with corresponding measurements made in various transonic tunnels with differences that could plausibly be explained as the effects of tunnel interference.

The effect of a simulated wind tunnel support sting is shown to increase the base pressure. The discrepancy between models with and without a sting is greatest at subsonic speeds and progressively decreases with increasing Mach number until at M = 1.4 the sting has no effect on base pressure.

The measured drag is in fair agreement with corresponding measurements made in various transonic tunnels with differences that could plausibly be explained as the effects of tunnel interference.

The effect of a simulated wind tunnel support sting is shown to increase the base pressure. The discrepancy between models with and without a sting is greatest at subsonic speeds and progressively decreases with increasing Mach number until at M = 1.4 the sting has no effect on base pressure.

The measured drag is in fair agreement with corresponding measurements made in various transonic tunnels with differences that could plausibly be explained as the effects of tunnel interference.

The effect of a simulated wind tunnel support sting is shown to increase the base pressure. The discrepancy between models with and without a sting is greatest at subsonic speeds and progressively decreases with increasing Mach number until at M = 1.4 the sting has no effect on base pressure.

Published by
HER MAJESTY'S STATIONERY OFFICE

To be purchased from
York House, Kingsway, London w.c.2
423 Oxford Street, London w.1
13A Castle Street, Edinburgh 2
109 St. Mary Street, Cardiff
39 King Street, Manchester 2
50 Fairfax Street, Bristol 1
2 Edmund Street, Birmingham 3
80 Chichester Street, Belfast 1
or through any bookseller

Printed in England

S.O. CODE No.23-9012-53